Modulation of laccase catalysed oxidations at the surface of magnetic nanoparticles

Lu Ren, Hongtao Ji, Karine Heuzé, Bruno Faure, Emilie Genin, Pierre Rousselot Pailley, Thierry Tron

Modulation of laccase catalysed oxidations at the surface of magnetic nanoparticles

Lu Ren,[a] Hongtao Ji,[b] Karine Heuzé,*[b] Bruno Faure,[a] Emilie Genin,[b] Pierre Rousselot Pailley[a] and Thierry Tron*[a]

a. Aix Marseille Université, Centrale Marseille, CNRS, iSm2 UMR7313, 13397 Marseille, France. Email : thierry.tron@univ-amu.fr.
b. Institut des Sciences Moléculaires, Université de Bordeaux, CNRS UMR5255, 33405 Talence cedex. Email : karine.heuze@u-bordeaux.fr

We explored the coupling of laccases to magnetic nanoparticles (MNPs) with different surface chemical coating. Two laccase variants offering two opposite and precise orientations of the substrate oxidation site were immobilised onto core-shell MNPs presenting either aliphatic aldehyde, aromatic aldehyde or azide functional groups at the particles surface. Oxidation capabilities of the six-resulting laccase-MNP hybrids were compared on ABTS and coniferyl alcohol. Herein, we show that the original interfaces created differ substantially in their reactivities with an amplitude from 1 to > 4 folds depending on the nature of the substrate. Taking enzyme orientation into account in the design of surface modification represents a way to introduce selectivity in laccase catalysed reactions.

Keywords: magnetic nano-particles; chemical coating; laccase orientation; oxidations

1-Introduction

The urgent requirement for a sustainable development of human society goes with environmental and economic issues that boost the development of catalysis. Regarding the increasing demand for environmentally friendly catalysis, biocatalysis is a blooming field. The catalyst (enzyme) itself is produced from readily available renewable resources, is biodegradable and essentially non-hazardous and nontoxic.[1] Enzymes do work under mild conditions (in water, at room temperature and atmospheric pressure), and generate little waste products. The sustainable development model displayed by enzyme-catalysed processes fits perfectly what is pursued in the present century.

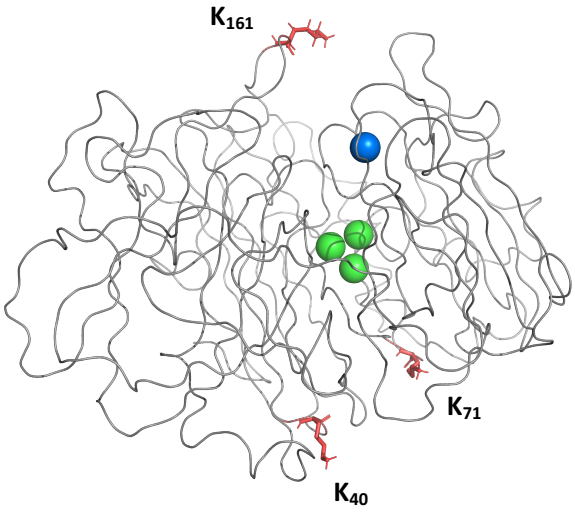

Figure 1: Model of the structure of the laccase LAC3 (Q6TH77) with three possible locations of lysine (side chain depicted in red) as they are present in the native enzyme (K_{71} and K_{40}) or in its $UNIK_{161}$ variant (K_{161}). Copper ions are depicted as colored spheres: blue (T1), green (TNC). View generated with PyMol (https://pymol.org/2/). Immobilization involving lysines of LAC3 will expose the T1 site to the solvent; immobilization involving the lysine of $UniK_{161}$ will expose the T1 site to the material surface. K is the one letter code for lysine (IUPAC amino acid code).

Laccases are multicopper enzymes.[2] They contain four copper ions distributed amongst two redox centres (Figure 1): a surface located mononuclear T1 copper near which substrate oxidation occurs and a trinuclear cluster (TNC) formed from a type 2 and type 3 copper ions, deeply embedded in the protein matrix where a four electrons reduction of molecular oxygen takes place. Due to the presence of these copper ions in their catalytic centres, laccases have the distinctive ability to couple the oxidation of a wide range of organic and inorganic compounds including substituted phenols (eq. 1), to the production of harmless water (eq. 2). Robust enzymes, laccases are useful for diverse biotechnological applications, such

as bio bleaching in the textile industry, lignin degradation in paper production, bioremediation processes, organic synthesis and for making bio-cathodes in biofuel cells.[3, , , , 7]

$$4\ \text{Ar-OH} \longrightarrow 4\ \text{Ar-O}^{\cdot} + 4\ \text{H}^{+} + 4\text{e}^{-} \quad \text{(eq.1)}$$

$$\text{O}_2 + 4\ \text{H}^{+} + 4\text{e}^{-} \longrightarrow 2\text{H}_2\text{O} \quad \text{(eq.2)}$$

In order to meet industrial requirements efforts are made to make laccase even stronger and more robust biocatalysts. Various cultivation techniques have been developed to efficiently produce laccase at the industrial scale.[8] Boosted yields and simplified purification process in laccase production are now available due to the development of robust heterologous expression systems.[9] Protein engineering offers the potential to tailor specific needs for efficient biocatalysts design.[10] Besides, the use of redox mediators allows extending laccase substrate range from phenolic compounds to non-phenolic compounds.[11] Additionally, immobilization of laccase on varieties of materials for different applications allows quick separation and easy recycling.[12]

A main difficulty for an extensive use of laccases for organic synthesis remains their lack of selectivity. Indeed, the mechanism by which these enzymes oxidize substrates is purely outer-sphere and does not require a properly defined substrate binding site at the enzyme surface.[13, 14] Therefore, *in vitro*, radical species issued from mono-electronic substrate oxidation (eq. 1) evolve independently of the enzyme. Molecular evolution techniques have been recently used to engineer laccase towards chemo-selectivity with some encouraging success.[15] Besides, few attempts have been made to introduce exogenously some selectivity in laccase catalysed reactions. For example, the laccase-TEMPO system is known for catalysing the regio-selective oxidation of the primary hydroxyl groups of sugar derivatives, allowing polymer functionalization.[16] Small organic cages like cyclodextrins have been shown to affect the fate of laccase mediated reactions.[17] To another extend, it is known that switching from one solvent to another can have a great influence on the selectivity of reactions catalysed by enzymes (substrate affinity, *ee*, regio and chemo selectivity).[18] In that direction, Danieli and coworkers described for the first time a significant and unexpected influence of the solvent on the relative ratio of two dimers obtained upon oxidative coupling of phenols catalysed by laccases.[19] Very recently, reports on bi-aryl coupling reactions suggest that some fungal laccases could be remarkably selective *in vivo*, in particular through the help of accessory proteins acting similarly to plant dirigent proteins (DIRs).[20]

Further to homogenous mixtures, exogenous materials brought close to the surface of enzymes during immobilization processes are recognized to substantially affect enzymes' properties.[21] However, beyond a commonly accepted role in improving enzymes' operational stability the interface between the protein, the material and the solvent is generally not well known. Yet, partitioning and mass transfer effects surely tune enzyme kinetics, optimal operational pH, as well as apparent substrate affinity and orientation. In the abundant literature devoted to laccase immobilizations, a control of the enzyme's orientation is consistently pursued in the elaboration of bio-cathodes.[22] In this case it is the optimization of the electron transfer which is pursued rather than reactivity at the surface of materials. As suggested by differences observed in the enantio-selectivity of an immobilised lipase depending on the nature of the support,[23] altering the microenvironment of a catalytic site at a material surface may represent a way to modulate enzymes selectivity. Taking enzyme orientation into account in the design of surface modification represents a potential to introduce (and control) further selectivity in laccase catalysed reactions.

Amongst all kinds of materials used for enzyme immobilization, superparamagnetic particles (MNPs) are one of the most popular.[24] Besides the convenience of a separation based on the use of a simple magnet, MNPs combine a high specific surface area and core-shell structures allowing to vary the reactive functional groups that cover the surface of the particles. Such surface variations make it possible to choose not only the immobilization method but also the micro-environment of the surface of the immobilised object. By playing both on the orientation of the enzyme during immobilization and on the nature of the functionalization layer, a modulation of the selectivity may be expected.[25] Here, we report on the covalent immobilization of a fungal laccase in two opposite orientations at the surface of core-shell MNPs offering three different functionalization layers. It is shown that, when the enzyme's active site is not part of the interface, laccase activity remains constant whatever the MNPs functional group is. To the contrary, varying MNPs surface chemical functions in the vicinity of the surface accessible active site of laccase directly influence its activity and beyond its selectivity.

2-Experimental

2.1-Materials

Unless otherwise stated, all chemicals and reagent used in the experiments were of analytical grade from commercial source. All chemicals and TurboBeads® click were purchased from Sigma-Aldrich and used as received. BcMag™ Beads were

purchased from Bioclone Inc. (San Diego, USA). MNP2 beads were synthesized from core-shell γ-Fe_2O_3/SiO_2, 300 nm superparamagnetic nanoparticles provided by Ademtech S.A, France (see below).

2.2-Custom synthesis of aldehyde activated particles (MNP2)

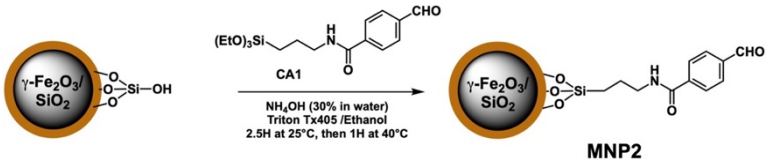

Scheme 1: Synthesis of MNP2

N-(3-triethoxysilylpropyl)-4-formyl benzamide (**CA1**) was synthesized according to Ahmadi et al.[26] To 10 mg of γ-Fe_2O_3/SiO_2 MNPs dispersed in a solution composed of 0.75 mL of 0.21 % Triton X-405 and 0.75 mL of ethanol a catalytic amount of 30 % NH_4OH (87 µL) was added. **CA1** (0.044 g, 0.125 mmol) dissolved in 0.5 mL of DMSO was then added dropwise over 2.5 hours to the suspension of particles under mechanical stirring (300 rpm) and under argon at 25°C. Afterwards, the suspension was stirred for 1 hour at 40°C. Finally, the particles were separated by magnetic decantation from the reaction medium, washed with 0.21 % Triton X-405 (5 × 1 mL) and stored at 4°C.
FT-IR analysis was performed on FT-IR Nicolet 6700 spectrometer equipped with DRIFT device (Fig. SI1). Custom made MNP2 were further characterized by TEM. As evaluated from this analysis, the grafting of CA1 resulted in an increase of the silica shell thickness of 6 nm compared to native particles (see Figure SI2 and Table SI1).

2.3-Physico-chemical characteristics of MNPs

MNPs characteristics are collected in Table 1. Density of grafts were determined by Fluorescence spectroscopy according to Yan et al. [27] for MNP2.

Table 1: MNPs characteristics[(a)]

	MNP1	**MNP2**[(b)]	**MNP3**
Diameter (m)	$1000\ 10^{-9}$	$300\ 10^{-9}$	$50\ 10^{-9}$
Specific area ($m^2\ g^{-1}$)	≈ 100	≈ 11	≈ 15
Particles per mass unit (g^{-1})	$1.7\ 10^{11}$	$4\ 10^{13}$	$2\ 10^{15}$ [(d)]
Density of graft (mol g^{-1})	$\approx 210\ 10^{-6}$	$\approx 1900\ 10^{-6}$	$\approx 100\ 10^{-6}$
Linker length (Å)[(c)]	24.3-25.8	11.5-12.5	14.1-14.3

(a): data obtained from manufacturers except otherwise specified; (b): data obtained in this study; (c): evaluated (calculation) from a simple model; (d) calculated value

2.4-Measurement of zeta potential

Zeta Potential measurements were carried out on Horiba Scientific nanoparticle analyzer SZ-100. The measurements were performed at 25°C for diluted aqueous suspension of MNPs at pH varying from 3.0 to 8.0 (Fig. SI3).

2.5-Laccases

The laccase LAC3 (from *Trametes* sp C30) and its variant $UNIK_{161}$ were produced in *Aspergillus niger* and purified as previously described.[32] Laccase concentration was estimated by UV-visible spectroscopy (Cary 60, Agilent Technologies, USA) using an $\varepsilon_{610\ nm}$ = 5600 $M^{-1}{\cdot}cm^{-1}$ for the T1 copper site. The molecular weight of the enzymes is MW≈ 80 000Da.

2.6-Enzyme immobilizations

Prior immobilization the storage buffer (20 mM phosphate buffer pH 6) was exchanged for the reaction buffer by concentration-dilution through a 30 kDa VIVASPIN 2 device (Sartorius Stedim Biotech, Germany) with 5~6 times repeat of centrifugation at 3000rpm 4°C. Magnetic particles were washed 3 times with Milli Q® water then suspended into the reaction buffer by vortexing vigorously for 1-2 minute (Aldehyde particles) or bathing in an ultrasonic bath for 20 min (Azide particles).

2.6.1-Immobilization to aldehyde particles

The procedure is adapted from the original procedure from MacFarland and Francis, 2005.[28] 2mg/mL magnetic particles, the appropriate amount of laccase (500 and 100 10^{-6} M final concentration respectively for MNP1 and MNP2) and 10 equiv. (relative to the enzyme concentration) of Iridium catalyst were mixed in a final volume of 200µL of Reductive Amination Buffer (50 10^{-3} M phosphate with 0.1 M sodium formate, pH 7.4) and incubated overnight at room temperature in a mixer (Eppendorf, Germany) with a continuous rotation (1000 rpm). The resulting laccase immobilised-MNPs were then obtained

by repeated cycles of washing and magnetic separation (controlling each time activity in the wash solution) and stored in Storage Buffer (0.1 M acetate buffer pH=5.7) at 4°C until use. The evolution of the immobilised laccase activity as function of the initial laccase concentration is given Figure 2 in the main text.

2.6.2-Immobilization to azide particles

$50\ 10^{-6}$ M (final concentration) of the appropriate laccase, 10 equiv. of 4-ethynylbenzaldehyde and Ir catalysts relative to the laccase concentration were mixed in a final volume of 2.5 mL Reductive Amination Buffer ($50\ 10^{-3}$ M aqueous phosphate with 0.1M sodium formate, pH 7.4) and slowly stirred under magnetic stirring for 72 hours at room temperature. After reaction, the resulting alkynylated enzymes were recovered by passing through a PD MiniTrap G-25 columns (Sigma Aldrich, France) and concentrated by ultrafiltration using a 30kD VIVASPIN 2 device (Sartorius Stedim Biotech, Germany).

Then, 10mg/mL azide particles, $1\ 10^{-6}$ M of alkynylated enzyme and 30 equiv. (relative to laccase concentration) of $CuSO_4$/Ascorbic acid/ bathophenanthrolinedisulfonic solutions were mixed in a final volume of Click buffer ($50\ 10^{-3}$ M Phosphate buffer pH=7.5). The mixture was stirred overnight at room temperature in a mixer (1000rpm/min). After reaction, particles were magnetically separated and the supernatant discarded. Particles were repeatedly washed/magnetically separated (controlling each time activity in the wash solution) and stored in Storage Buffer (0.1M acetate buffer pH=5.7) at 4°C until use. The evolution of the immobilised laccase activity as function of the initial laccase concentration is given Figure SI4.

2.7-Enzyme loading evaluation (Elisa)

The detailed procedure can be found in Zhou et al., 2018;[29] the entire process of ELISA employed in this study is depicted Figure SI5.
Coating buffer: 0.2 M sodium carbonate/bicarbonate, pH 9.4; Washing buffer: 0.1 M phosphate, 0.15 M sodium chloride, pH 7.2 containing 0.05% Tween 20; Blocking buffer: 2% (w/v) Bovine Serum Albumin (BSA) in Washing Buffer; Substrate solution: 1 tablet of PNPP (Sigma S0942) dissolve into 10 mL Glycine buffer (0.1 M glycine, pH 10.4, with $1\ 10^{-3}$ M $MgCl_2$ and $1\ 10^{-3}$ M $ZnCl_2$).
Briefly, standard enzyme samples with different concentrations and the immobilised enzyme samples were added to a microplate, in a final volume of 100 µL in each well; the microplate was then covered and incubated at room temperature for 2 hours or at 4 ℃ overnight. Supernatants were removed (the microplate was held on a magnetic stand when discarding the supernatant) and the wells washed 3 times with 200 µL of washing buffer. Subsequently, blocking buffer (300 µL) was added to each well and the microplate was then covered and incubated under agitation at 600rpm for 1 hour at room temperature. After disposal of the blocking buffer (with the help of the magnetic stand), 100 µL of the biotinylated detection AC (anti LAC3, 5000× dilution with blocking buffer) was added per well and the microplate was covered and incubated under agitation at 600rpm for 1 hour at room temperature. Supernatants were discarded and the wells washed 5 times with 200µL of washing buffer. Next, 100 µL of the enzyme conjugate Alkaline Phosphatase-streptavidin (1000× dilutions with washing buffer) was added to each well and the covered microplate further incubated under agitation at 600rpm for 1 hour at room temperature. Supernatants were again discarded and the well washed 7 times with washing buffer. Eventually, 100 µL of substrate (PNPP) solution was added to each well and the plate was incubated at RT until color developed. Absorbance of PNP was read at 405nm with a plate reader. Standard curves based on measured absorbance values were established allowing to calculate enzyme loadings (Fig. SI6).

2.8-Theoretical evaluation of enzyme loads

Efficiency of grafting depends on the MNP's specific area, on the number of function available for grafting and on the efficiency of the coupling reaction. The following calculations are given to provide theoretical numbers (maxima) to compare with experimental values of enzyme grafting. Data on MNPs are taken from Table 1. Projection of the enzyme (Ø ≈ 4 – 5nm) on a surface: $\pi r^2 = 1.3 - 2\ 10^{-17}\ m^2$; $\mathcal{A} = 6.023\ 10^{23}\ mol^{-1}$ (Avogadro number).
MNP1: $(100\ m^2\ g^{-1} / 1.3 - 2\ 10^{-17}\ m^2 / \mathcal{A}) \approx 8 - 13\ 10^{-6}\ mol\ g^{-1}$
Note: taking into account the specific area and the number of particles per mass unit given Table 1 the bead's surface is calculated to be: $100 / 1.7\ 10^{11} = 5.9\ 10^{-10}\ m^2$. This value appears surprisingly high for 1000 nm beads with a smooth surface ($4\pi r^2 = 3.1410^{-12}\ m^2$) suggesting a rough silica shell greatly extending the surface available to grafting.
MNP2: $(11\ m^2\ g^{-1} / 1.3 - 2\ 10^{-17}\ m^2 / \mathcal{A}) \approx 1 - 1.5\ 10^{-6}\ mol\ g^{-1}$
MNP3: $(15\ m^2\ g^{-1} / 1.3 - 2\ 10^{-17}\ m^2 / \mathcal{A}) \approx 1.2 - 2\ 10^{-6}\ mol\ g^{-1}$

2.9-Laccase activity measurements

2.9.1-ABTS oxidation

The mono-electronic oxidation of ABTS results in the formation of a stable emerald green radical cation ($ABTS^{+\bullet}$).
Activities of the free and immobilised laccase were determined against 2,2'-azino-bis (3-ethylbenzthiazoline-6-sulphonic acid) (ABTS) in 0.1 M of Acetate buffer pH 5.5 at 30°C. Formation of the cation ($\varepsilon_{420\ nm}$ =36000 $M^{-1}\cdot cm^{-1}$, calculation factor 27.8) was followed for 2 min using a spectrophotometer (Cary 60, Agilent Technologies, USA).

For the measurement of the free laccase activity, 10 µL of the appropriately diluted enzyme samples was added into 890 µL of 0.1 M of Acetate buffer pH 5.5 at 30°C; the enzymatic reaction was started by adding 100 µL ABTS solutions (50 10^{-3} M) into the reaction mixture. For the determination of the immobilised laccase activity, the reaction contained 10 µL of MNP-immobilised laccase suspension (20 µg of particles at 2 mg/ml concentration), 890 µL of 0.1 M Acetate buffer pH 5.5 (pre-heated to 30°C in a water bath), and 100 µL ABTS solutions (50 10^{-3} M). The amount of laccase oxidizing one micromole of substrate per minute is defined as one unit (U). All the experiments were carried out as triplicates and all results presented are average of triplicates.

2.9.1-Coniferyl alcohol oxidation

Laccases oxidize coniferyl alcohol generating a resonance stabilized 4-vinylphenoxyl radical ($CA^{\bullet}$) which dimerises (random coupling) to form the (±) pinoresinol (PINO), (±) dehydrodiconiferyl alcohol (DHCA) and (±) erytro/threo guiacylglycerol (GUA) dimers (Scheme SI1). Oxidations of coniferyl alcohol (CA) catalysed by free and immobilised laccase were carried out in a 2 ml centrifuge tubes. All experiments were performed in 0.1 M acetate buffer, pH 5,5. The final concentration of CA was 1.6mM; the amount of laccase used was variable depending on the experiment (generally 1U/L as measured with ABTS). A thermomixer set at 30 °C and 1000 rpm was used for the incubation. Samples were taken out at given time points and the reaction was stopped by addition of 1 volume of an acetonitrile solution of benzophenone (benzo: internal reference for HPLC). For the immobilised laccase samples, particles were captured with a magnet prior injection onto the HPLC column for analysis. HPLC analysis were carried out with a JASCO LC-4000 series HPLC (JASCO, Japan). Samples were separated on a reverse phase Nucleosil 100-5 C18 column (Macherey-Nagel, Germany) with a mobile phase composed of a mixture of water - acetic acid 3% (solvent A) and acetonitrile (solvent B) with the following gradient: 90% A 10 % B for 5 min then 10% solvent B to 50% in 20 min then plateau 50% solvent B for 2 min then back to 10% solvent B for 2 min (Fig. SI7).

Results and discussion

Design of the laccase/MNP interface.

Demonstrations of targeted orientations of a fungal laccase at a material surface have been previously obtained for example on functionalized carbon nanotubes.[30] LAC3 from *Trametes* sp. C30 is a typical fungal laccase produced in high yield as a recombinant enzyme.[31] Its sequence contains naturally only two lysines, K_{40} and K_{71}, out of 501 residues. LAC3 is our reference enzyme for the creation of variants, called UNIKs, with a unique surface accessible lysine residue.[32] Here, we selected $UniK_{161}$ (K_{40}->M, K_{71}->H, R_{161}->K) the unique lysine side-chain of which is offering a single free reactive -NH_2 group for a functionalization nearby the T1 copper site while the two natural free -NH_2 groups of LAC3 are offering the potential of a dual surface functionalization diametrically opposed to the T1 copper site with respect to the TNC (Figure 1). These laccase variants can be efficiently functionalized via a reductive alkylation of their discrete lysine groups in a reaction adapted from Mc Farland and Francis.[33] Neither the surface mutations (K_{40}->M, K_{71}->H, R_{161}->K) nor a subsequent lysine functionalization lead to a significant modification of the catalytic efficiency of enzymes.[30, 32]

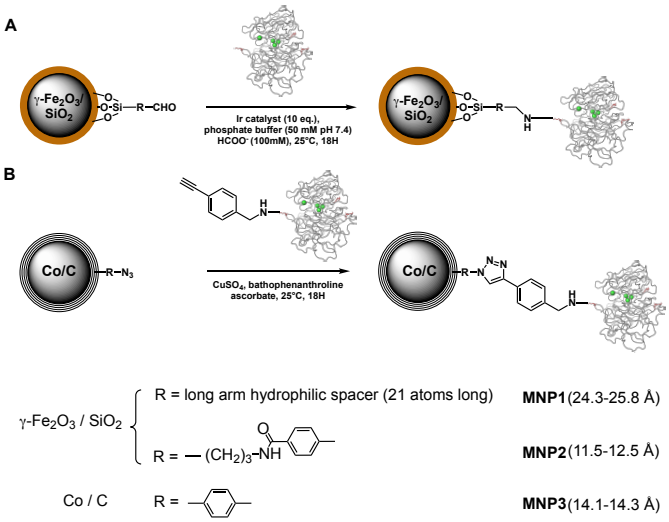

Scheme 2: Grafted core-shell MNPs. A: reductive alkylation; iron-oxide core/silica shell aldehyde particles; MNP1 = long arm hydrophilic spacer, MNP2 = aromatic spacer. B: azide-alkyne cycloaddition; cobalt core/carbon layers shell azido particles (MNP3); alkyne activated laccase (reductive alkylation). Approximative lengths of linkers (enzyme-to-shell) are given in brackets.

In order to modulate the physicochemical properties of the interface, MNPs with different surface functional groups were selected for a covalent immobilization of the two laccase variants. Given the reactivity of the enzyme's lysine groups, aldehyde-activated MNPs were targeted in the first place (Scheme 2A). Hence, the BcMag™ Beads from Bioclone that are functionalized with an aldehyde group ending a long hydrophilic spacer (MNP1) and custom benzaldehyde activated γ-Fe_2O_3/SiO_2 particles. On the other hand, providing a surface lysine is first activated with an alkyne (or azide) group, laccase enzymes can be engaged in an alkyne-azide *Huisgen* 1,3-dipolar cycloaddition with no significant loss of activity.[30] Therefore, TurboBeads® click (MNP3) were chosen for the immobilization of variants via click chemistry (scheme 2B). For each MNP, the pH dependency of the zeta potential was evaluated from aqueous suspensions (Fig. SI3). Physicochemical characteristics of the chosen MNPs are given in Table 1.

For both the reductive alkylation and the cycloaddition the selectivity of the functionalization reaction prevents the reaction of non-lysine groups present on the protein surface with particles. After functionalization, particles were extensively washed with a buffered solution to remove non-covalently bound enzymes. The resulting six different laccase/MNPs hybrids were then compared for their ability to oxidize two different substrates, i.e. the synthetic substrate ABTS (2, 2'-azinobis (3-ethylbenzothiazoline-6-sulfonic acid) and the natural substrate coniferyl alcohol (3-(4-Hydroxy-3-methoxyphenyl)-2-propen-1-ol). Rather different in their structures (Scheme 3) these laccases substrates are proposed to interact with different areas at the enzyme surface.[34]

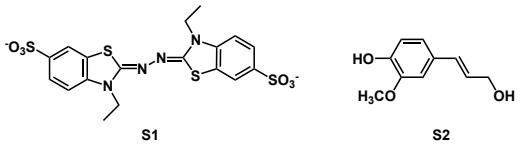

Scheme 3: Laccase substrates. **S1**: ABTS (2, 2'-azinobis (3-ethylbenzothiazoline-6-sulfonic acid); **S2**: coniferyl alcohol (3-(4-Hydroxy-3-methoxyphenyl)-2-propen-1-ol).

Determination of initial laccase concentration for the oriented immobilization of laccase

The immobilization process was studied using LAC3 as a model enzyme. Evolution of the immobilised laccase activity (ABTS as substrate) as function of the initial laccase concentration used in the immobilization process is given Figure 2 for MNP1 and MNP2. As previously reported for other laccase-MNP hybrids,[35] for both particles, the activity of the immobilised laccase increased linearly with the initial laccase concentration before reaching a plateau here from respectively 500 10^{-6} M of enzyme for MNP1 and 100 10^{-6} M for MNP2. For MNP3 this plateau is reached at much lower concentration (10^{-6} M), so the initial laccase concentration used was ranging from 1 to 10 10^{-6} M (Fig. SI4). A plateau is usually interpreted as a "saturation", that could here apply either to the grafts or to the surface of the particles. Therefore, in subsequent immobilization experiments initial laccase concentration was set to the value at which a plateau is reached, i.e. 100 10^{-6} M for MNP1, 500 10^{-6} M for MNP2 and 10^{-6} M for MNP3.

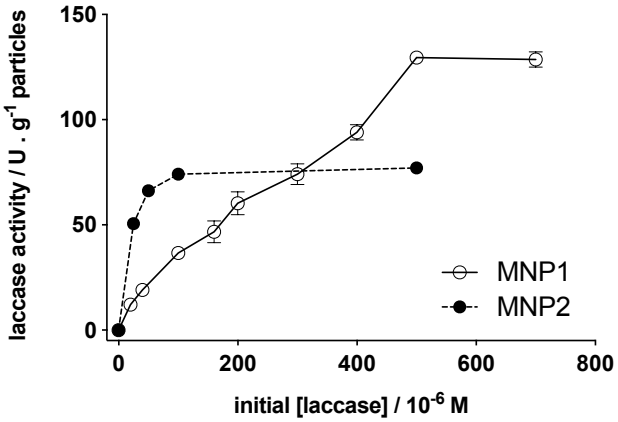

Figure 2: Initial laccase concentration *versus* immobilised laccase activity. MNP1 and MNP2 particles concentration 2 $g.L^{-1}$ incubated at 30°C in 0.1 M acetate buffer pH 5.5 in the presence of ABTS (5 10^{-3} M final). Kinetics of the radical cation formation followed spectrophotometrically at 420 nm (ε= 36 000 mol^{-1} cm^{-1}) for 2 min.

Hybrids activities appear consistent with results reported in literature.[36] However, multilayers or clusters of enzyme molecules resulting from protein-protein interaction at the surface of the support may occur.[37] When enzyme molecules

are densely packed in multi-layers mass-transfer limitation results in a reduction of the activity of the immobilised enzymes.[38] Then, consequences of the orientation of laccase on particles surface on its activity could be blurred. Therefore, to be able to compare the effect of oriented immobilization on laccase activity, the concentration contributing to the maximum activity of immobilised laccase should be determined first to reduce the influence of high density or multilayer coverage at the greatest extent.

Enzyme loading

Enzyme loading is usually evaluated from a comparison of the concentration of proteins in solution before and after immobilization. In the case of laccase, besides classical spectrophotometric (A_{280}) or indirect colorimetric (e.g. Bradford) assays, an intense Cys(S)⇒Cu^{II} charge transfer band in the absorption spectrum of the oxidized enzyme (ε ≈ 5000-6000 M^{-1} cm^{-1} at about 600 nm) can be used to determine the concentration. However, none of these assays were found practical here principally because working with diluted solutions, protein concentrations are close to detection limits. Therefore, we rather used an Enzyme Linked Immuno Sorbent Assay (ELISA) to quantify the amount of enzyme grafted onto MNPs (see detailed procedure in SI). Commonly used for free proteins, ELISA may not be that frequently used for immobilised enzymes quantification. It is then worth going through some experimental details to highlight its appropriateness in this case.

In this assay, LAC3-MNPs (antigens) first adsorbed to the wells of a microplate are complexed by a biotinylated anti-LAC3 antibody and tagged with a streptavidin-alkaline phosphatase for ultimate detection (Fig. SI5). The colorimetric titration of product formation typically corresponds to a detection level in the range of picogram of antigen per well. Three independent immobilizations of LAC3 and $UniK_{161}$ performed on each MNP were tested to evaluate enzyme loadings. Freshly produced $UniK_{161}$ was used as standard enzyme for establishing calibration curves. For each measurement, two different amounts of grafted MNPs were evaluated and the corresponding amounts of bare particles used as blank controls. Standard samples and grafted MNP samples were tested in triplicate in a microwell plate. Curves depicting the relationship between the absorbance of the end product at 405nm and the concentration of protein are shown in Figure SI6. Sampled MNPs are within the working range of the curves. Product formation increases proportionally with the increase of particle amount. As bare particles have no absorbance themselves (i.e. residual absorbance equivalent to that of the protein blank) this increase in product formation correlates with amounts of immobilised enzymes in the well. Averaged enzyme loadings are given Table 2.

Table 2. Amounts of enzyme grafted on the different MNPs (enzyme loading). Each value represents the mean of triplicates for two different amounts of particles.

	MNP1 (10^{-3}g/g)		**MNP2 (10^{-3}g/g)**		**MNP3 (10^{-3}g/g)**	
	LAC3	$UNIK_{161}$	LAC3	$UNIK_{161}$	LAC3	$UNIK_{161}$
I1	150	174	89	89	1.4	1.7
I2	187	165	92	90	2.5	2.4
I3	132	129	87	102	2.1	1.4

For each MNP, deviations observed for the three independent immobilizations (I1, I2, I3) are relatively small considering the nature of the materials. Relative to each other, loads achieved are comparable for MNP1 and MNP2 and 1 to 2 orders of magnitude lower for MNP3. Efficiency of enzyme immobilization depends on the MNP's specific area, on the number of function available for grafting and on the efficiency of the coupling reaction. In view of their respective physicochemical properties (Table 1), data from Table 2 highlight differences of grafting efficiencies for each MNP. Comparing experimental values to an estimate of the maximum theoretical occupancy per particle unit (obtained relating the projected area of the enzyme to the surface of the particle, see Experimental section for calculations), grafting efficiencies are evaluated to be 15 –25 %, 80 – 100 % and 1 – 2 % respectively for MNP1, MNP2 and MNP3(using a Mw≈80 000 Da for the enzymes). For MNP2, the efficiency of the reductive alkylation reaction appears maximum and this correlates well with the saturation observed earlier when varying the enzyme concentration (*vide supra*). On the other hand, for MNP1 the efficiency of the coupling reaction is much lower and that despite MNP1 and MNP2 were grafted in the very same conditions. With an amount two orders of magnitude higher than the estimated amount of grafted enzyme, availability of aldehyde group at the surface of the MNP1 particles is not a limiting factor. Therefore, the relative decrease in efficiency of the coupling reaction observed for MNP1 may be principally related to a lower reactivity of aliphatic aldehyde groups compared to aromatic ones. Compared to the Cu promoted click reaction the reductive alkylation appears however particularly efficient. Anyway, whatever the functionalization mode, it is noteworthy that enzyme orientation does not seem to influence the grafting efficiency. This pre-requisite verified, activities of MNPs with opposite orientations of enzymes were then compared.

Activity of immobilised laccases

Oxidation of ABTS. The mono-electronic oxidation of ABTS results in the formation of a stable emerald green radical cation ($ABTS^{\bullet+}$). The kinetic of ABTS oxidation was followed in stirred solutions containing either a free laccase (LAC3 or $UniK_{161}$) or a laccase-MNP hybrid (2 $g.L^{-1}$) derived from three independent immobilizations of LAC3 and $UniK_{161}$ performed on each MNP. For each immobilization, free LAC3 or $UniK_{161}$ activity per milligram of total protein, i. e. their specific activity (SA), was similar (from 70 to 170 $U.mg^{-1}$ depending on batches). SA of the different batches of laccase-MNP hybrids is compared Figure 3.

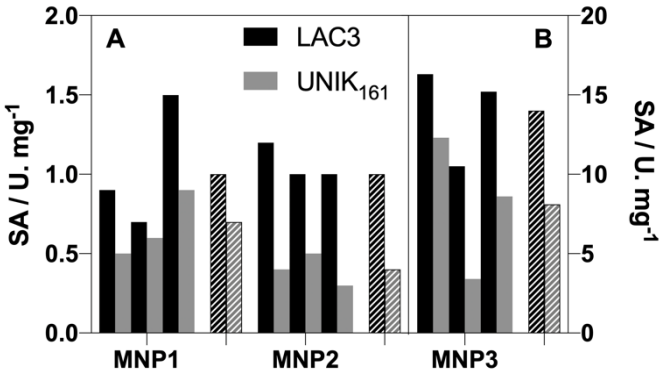

Figure 3: Specific activity of laccase-MNP hybrids towards ABTS. For each MNP, comparison of three sets of particles (I1 to I3 from Table 2) independently grafted either with LAC3 or $UniK_{161}$. A: aldehyde functionalized particles; B: azide functionalized particles. Laccase-MNP hybrids (2 $g.L^{-1}$) incubated at 30°C in 0.1 M acetate buffer pH 5.5 in the presence of ABTS (5 mM final). Kinetics of the radical cation formation followed spectrophotometrically at 420 nm (ε= 36 000 mol^{-1} cm^{-1}) for 2 min. Each value represents the mean of three independent measurement related to the mass of protein (from Table 2). Dashed bars correspond to the mean of each subset.

Despite of a slight heterogeneity in results from the immobilization subsets (I1 to I3), SA of LAC3-MNP hybrids is consistently higher than that of $UniK_{161}$-MNP hybrids and that whatever the nature of the particle. This is consistent with results we have recently obtained on the decolourization of dye models with laccase variants oriented at the surface of silica foams.[39] This trend highlights a general effect exerted by the surface of materials on the oxidation site of the enzyme. Corrected from the bias of initial SA of the free enzymes used for immobilization, the ratio LAC3/$UNIK_{161}$ range from 1.7 to 2.7 (Table 3). Related examples of site-directed orientation studies can be found in literature with enzymes as different as lipase,[40] glucose-6-phosphate dehydrogenase,[41] pyrophosphatase,[42] or β-galactosidase.[43] For these enzymes that have structurally defined active sites, the relative loss of enzyme activity (i.e. the ratio of activities of variants with active sites solvent exposed/material exposed) is more or less pronounced, a variation that might be primarily related to the bulkiness of their respective substrates. At the pH of the reaction all three MNPs are negatively charged particles (see SI for zeta potential measurements). Moreover, it is reasonable to think that the negative electrostatic contribution of the enzyme to the overall charge of the surface of the particle can only strengthen this negatively charged surface. This likely provides a repulsive environment for a negatively charged ABTS substrate.[44] On the other hand, in laccase substrate oxidation is an outer sphere mechanism (i.e. there is no coordination of the substrate to the metal) and there is not a truly defined substrate binding site. Therefore, it is tempting to think that the weight of factors like the limitation of diffusion at the liquid/solid interface and steric hindrance may here prevail on that of a deformation of the "active site".

Table 3. Ratios of the specific activity (ABTS) of enzymes grafted on the different MNPs.

	LAC3 / $UNIK_{161}$		
	MNP1	**MNP2**	**MNP3**
Free enzymes[a]	0.8	1.0	1.0
I1	1.7	2.8	1.3
I2	1.2	2.3	3.0
I3	1.7	3.2	1.8
Mean	1.9[a]	2.7	1.7

[a] SA from 70 to 170 U mg^{-1} depending on batches of enzymes; b corrected from the bias of the initial SA of free enzymes.

Given the different spacers we used (scheme 2), the distance from the enzyme surface to the functionalization crown is expected to vary from one grafting to another (calculated to be ≈ 11 to 26 Å, scheme 2). It is generally considered that a short linker conveys more rigidity to the system whereas a longer linker reduces steric hindrance. Comparing SA ratios of the enzymes grafted on MNP1 and MNP2, these constructions seem to comply with this consideration (Table 3). However, it is probable that any "length effect" is here compensated because of the difference of diameter (i.e. 1000 10^{-9} m for MNP1 and 300 10^{-9} m for MNP2) and therefore of curvature of the particles.[45] On the other hand, despite an enzyme-to-shell distance about 20% longer than for MNP2 as well as a curvature 20 times more pronounced than for MNP1, the SA ratio of LAC3 vs $UniK_{161}$ grafted MNP3 still remains substantially above 1 (Table 3). Therefore, factors tuning the oxidation of the voluminous ABTS include charge and variations of the chemical environment of the oxidation site modulated by the length and the hydrophilic or hydrophobic character of the linker and the nature of the terminal function.

Oxidation of coniferyl alcohol. Coniferyl alcohol (CA) belongs to the monolignol family of plant secondary metabolites.[46] Compared to ABTS, CA is smaller (8.6 Å vs 17 Å), neutral, hydrophobic. Laccases oxidize coniferyl alcohol generating a resonance stabilized 4-vinylphenoxyl radical ($CA^{\bullet+}$) which dimerises to form the (±) pinoresinol (PINO), (±) dehydrodiconiferyl alcohol (DHCA) and (±) erytro/threo guiacylglycerol (GUA) dimers (scheme SI1). DHCA is the major product amongst the three dimers.

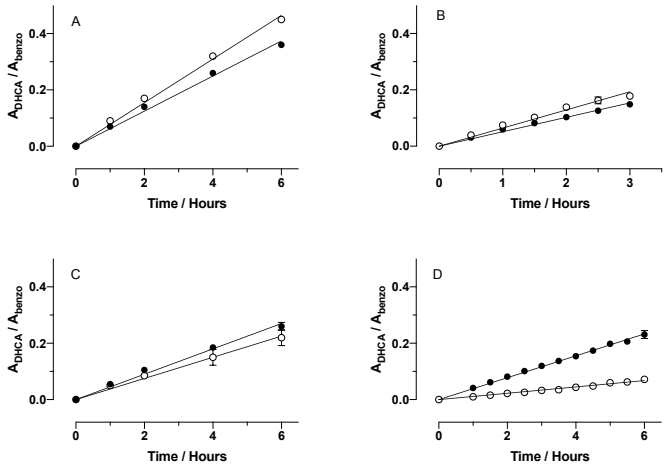

Figure 4: Influence of laccase-MNP hybrids on (±) dehydroconiferyl alcohol (DHCA) production. Laccase-MNPs (accounting for the same final concentration of LAC3 or $UniK_{161}$) incubated at 30°C in 0.1 M acetate buffer pH 5.5 in the presence of coniferyl alcohol (CA, 1.6 10^{-3} M). The appearance of DHCA (the major CA oxidation product) was followed by HPLC as function of time. Y axis: the peak area of DHCA normalized to the peak area of benzophenone (1 10^{-3} M) used as internal standard. A: free enzymes; B: Laccase-MNP3; C: Laccase-MNP1; D: laccase-MNP2. LAC3, closed symbol, $UNIK_{161}$, open symbol. Error bars represent standard deviation on three replicates. Dashed lines are linear regression of data.

Substrate consumption and coupling products formation in the presence of the different laccase-MNP hybrids were monitored by HPLC (Fig. SI6). For each experiment, concentrations of LAC3 and UNIK were kept identical and adjusted in order to prevent a rapid exhaustion of the CA substrate. Dimers being oxidizable as well, a low laccase concentration and an excess of CA reduced the bias introduced by concurrent kinetics.[17] In an initial control experiment, with a ratio of slopes $LAC3/UNIK_{161}$ = 0.8, DHCA production appeared slightly faster with free $Unik_{161}$ than with free LAC3 (Fig.4A) and that despite of the use of an identical concentration of enzymes with a similar SA on ABTS (ratio ≈ 1). This small difference may be related to the variation of amino-acid at position 161 since this amino acid is located in an area of the enzyme surface to which phenolic substrates but not ABTS appears to interact with.[34]

Laccase-MNP hybrids DHCA production kinetics are presented Figure 4. Amongst the six hybrids tested, the activity of laccase-MNP3 hybrids appears clearly independent of the enzyme orientation. Indeed, using the same amount of LAC3 and $Unik_{161}$ enzymes (as laccase-MNP hybrids) DHCA production proceeds with similar rates (Fig. 4B) with a ratio of slopes $LAC3/UNIK_{161}$ ≈ 1 if one takes into account the bias observed for control homogenous reactions (Fig. 4A). Therefore, contrary to what was previously observed with ABTS for these hybrids, the local microenvironment of the oxidation site has apparently no influence on the oxidation of the small hydrophobic and neutral CA substrate. On the other hand, DHCA production rates are clearly influenced by the orientation of the enzyme at the particle surface and in a differentiated way

for the laccase-MNP1 and laccase-MNP2 hybrids (Fig. 4C, D). Indeed, the ratio of slopes LAC3/UNIK$_{161}$ vary from≈ 1.5 (laccase-MNP1 hybrids) to > 4 (laccase-MNP2 hybrids). In the absence of the electrostatic effect earlier invoked with ABTS this is a surprisingly marked difference of activity for the UNIK$_{161}$-MNP2 hybrid. As argued before, effects expected from variations of the length of the linker or that of the curvature of the particle are exerted in an opposite way in our constructions. On the other hand, with a small hydrophobic substrate as CA, the hydrophilicity vs hydrophobicity of linkers in MNP1 and MNP2 constructs could be discriminant, which does not seem to be the case in a first analysis. Still, this may apply here while being overwhelmed by the amplitude of another effect, steric for example. Actually, this amplitude may be a consequence of the presence of a benzaldehyde moiety in the grafting linker of the MNP2 particle (Scheme 1). Indeed, resembling a laccase phenolic substrate, it is conceivable that such a free grafting function could increase steric hindrance near the enzyme's oxidation site therefore gating the substrate accessibility. Globally, as studied in laccase-MNP hybrids, it appears that laccase activity can be modulated directly by the functionalization layer. Experiments are ongoing in our laboratories to further investigate on these interfacial effects.

Conclusions

We achieved the construction of laccase-(core/shell) magnetic nanoparticles hybrids with different catalytic properties. The precise orientation of the enzyme at the MNPs surface allowed probing the impact of the local environment on laccase activity. Hence, the choice of functionalization layers modulating surface chemical properties of the support to which the oxidation centre located at the surface of enzyme molecules is directly exposed to. With the very same enzyme, we achieve three original interfaces with substantial differences of reactivity the amplitude of which is depending on the nature of the substrate. Beyond consequences expected from varying physical parameters like here the curvature of the particle or the length of the linker, variations of chemical functions in the immediate vicinity of the substrate oxidation appear as a fine tool for the modulation of laccase activity in hybrid biocatalysts. Although immobilization technologies are primarily used for the stabilization and recyclability of enzymes, our results advocate for a careful construction of a structured chemical landscape around the substrate oxidation site. Combined to molecular evolution of the enzyme this should help to design new functions for laccase-hybrid systems.

Conflicts of interest

"There are no conflicts to declare".

Acknowledgements

This study was supported by funds from the CNRS, Aix Marseille Université (AMU), University of Bordeaux and partly from a grant from the Agence Nationale de la Recherche (ANR-15-CE07-0021-01). L.R. and H. J. acknowledge funding from China Scholarship Council for their PhD grant (Files No. 201604490005 and No. 201706130132 respectively). We thank Ademtech SA. for providing γ-Fe_2O_3/SiO_2 nanoparticles. We thank C. Aupetit for the access to FT-IR DRIFT and Etienne GONTIER from the Bordeaux Imaging Center for the help in acquiring TEM images. We thank Elise Courvoisier-Dezord from the Plateforme AVB (AMU): Analyse et Valorisation de la Biodiversité and Yolande Charmasson for help in the production of recombinant laccases. We also thank Dr. Ariane Jalila Simaan for numerous stimulating discussions.

Appendix A. Supplementary data

FTIR spectrum of MNP2; TEM images of MNP2; Zeta potentials; Laccase concentration dependency in MNP3 preparations; Elisa tests; Oxidation of coniferyl alcohol; References. See DOI:

References

1 R. A. Sheldon and J. M. Woodley, *Chemical reviews*, 2017, **118**, 801–838.
2 T. Tron in *Encyclopedia of Metalloproteins* (Eds.: R. H. Kretsinger, V. N.Uversky, E. A. Permyakov), Springer, New York, 2013, pp. 1066 –1070.
3 R. A. Abd El Monssef, E. A. Hassan and E. M. Ramadan, *Annals of Agricultural Sciences*, 2016, **61**, 145–154.
4 A. Bronikowski, P.-L. Hagedoorn, K. Koschorreck and V. B. Urlacher, *AMB Express*, 2017, **7**, 73.
5 F. Darvishi, M. Moradi, C. Jolivalt and C. Madzak, *Ecotoxicology and environmental safety*, 2018, **165**, 278–283.
6 C. Ji, J. Hou, K. Wang, Y. H. Ng and V. Chen, *Angew. Chem. Int. Ed.*, 2017, **56**, 9762–9766.
7 J. Sun, N. Guo, L.-L. Niu, Q.-F. Wang, Y.-P. Zang, Y.-G. Zu and Y.-J. Fu, *Molecules*, 2017, **22**, 673.

8 K. Brijwani, A. Rigdon and P. V. Vadlani, *Enzyme Research*, 2010, **2010**, 1–10.
9 M. Ayala, M. A. Pickard and R. Vazquez-Duhalt, *J Mol Microbiol Biotechnol*, 2008, **15**, 172–180.
10 C. J. Rodgers, C. F. Blanford, S. R. Giddens, P. Skamnioti, F. A. Armstrong and S. J. Gurr, *Trends in Biotechnology*, 2010, **28**, 63–72.
11 O. V. Morozova, G. P. Shumakovich, S. V. Shleev and Y. I. Yaropolov, *Applied Biochemistry and Microbiology*, 2007, **43**, 523–535.
12 M. Fernández-Fernández, M. Á. Sanromán and D. Moldes, *Biotechnology Advances*, 2013, **31**, 1808–1825.
13 R. Mehra, J. Muschiol, A. S. Meyer and K.P. Kepp, *Scientific Reports*, 2018, **8**, 1-16.
14 S. Riva. *Trends Biotechnol.*, 2006, 24, 219-26.
15 G. Santiago, F. de Salas, M. F. Lucas, E. Monza, S. Acebes, Á. T. Martinez, S. Camarero and V. Guallar, *ACS Catal.*, 2016, **6**, 5415–5423.
16 M. Fabbrini, C. Galli, P. Gentili and D. Macchitella, *Tetrahedron Letters*, 2001, **42**, 7551–7553.
17 L. Tarrago, C. Modolo, M. Yemloul, V. Robert, P. Rousselot-Pailley and T. Tron, *New Journal of Chemistry*, 2018, **42**, 11770–11775.
18 A. M. Klibanov, *Nature*, 2001, **409**, 241–246.
19 A. Intra, S. Nicotra, S. Riva and B. Danieli, *Advanced Synthesis & Catalysis*, 2005, **347**, 973–977.
20 W. Thiele, S. Obermaier and M. Müller, *ACS Chem. Biol.*, 2020, **15**, 844–848.
21 J. N. Talbert and J. M. Goddard, *Colloids and Surfaces B: Biointerfaces*, 2012, **93**, 8–19.
22 Ievgen Mazurenko, Vivek Pratap Hitaishi, Elisabeth Lojou, *Current Opinion in Electrochemistry*, 2020, **19**, 113-121.
23 C. Mateo, J. M. Palomo, G. Fernandez-Lorente, J. M. Guisan and R. Fernandez-Lafuente, *Enzyme and Microbial Technology*, 2007, **40**, 1451–1463.
24 a) R. G. Chaudhui and S. Paria, *Chem. Rev*., 2012, 112, 2373-2433; b) R.A. Bohara, N. D. Thorat and S. H. Pawar, *RSC Advances*, 2016, **6**, 43989-44012.
25 O. Barbosa, R. Torres, C. Ortiz, Á. Berenguer-Murcia, R. C. Rodrigues and R. Fernandez-Lafuente, *Biomacromolecules* 2013, **14**, 2433–2462.
26 E. Ahmadi, A. Ramazani, A. Mashhadi-Malekzadeh, Z. Hamdi and Z. Mohamadnia*, Bull. Mater. Sci.* 2014, **37**, 1101-1112.
27 B. Yan and W. Li, *J. Org. Chem*. 1997, **62**, 9354-9357.
28 J. M. McFarland, M. B. Francis, *J. Am. Chem. Soc*. 2005, **127**, 13490-13491.
29 S. Zhou, P. Rousselot-Pailley, L. Ren, Y. Charmasson, E. Courvoisier Dezord, V. Robert, T. Tron and Y. Mekmouche, Methods in Enzymology, 2018, **613**, 17-61.
30 a) N. Lalaoui, P. Rousselot-Pailley, V. Robert, Y. Mekmouche, R. Villalonga, M. Holzinger, S. Cosnier, T. Tron and A. Le Goff, *ACS Catal.*, 2016, **6**, 1894–1900, b) S. Gentil, P. Rousselot-Pailley, F. Sancho, V. Robert, Y. Mekmouche, V. Guallar, T. Tron and A. Le Goff, *Chem. Eur. J.*, 2020, **26**, 4798–4804.
31 a) A. Klonowska, C. Gaudin, M. Asso, A. Fournel, M. Réglier and T. Tron, *Enzyme and Microbial Technology*, 2005, **36**, 34–41; b) Y. Mekmouche, S. Zhou, A. M. Cusano, E. Record, A. Lomascolo, V. Robert, A. J. Simaan, P. Rousselot-Pailley, S. Ullah, F. Chaspoul and T. Tron, *Journal of Bioscience and Bioengineering*, 2014, **117**, 25–27.
32 V. Robert, E. Monza, L. Tarrago, F. Sancho, A. De Falco, L. Schneider, E. Npetgat Ngoutane, Y. Mekmouche, P. R. Pailley, A. J. Simaan, V. Guallar and T. Tron, *ChemPlusChem*, 2017, **82**, 607–614.
33 J. M. McFarland and M. B. Francis, *J. Am. Chem. Soc.*, 2005, **127**, 13490–13491.
34 a) T. Bertrand, C. Jolivalt, P. Briozzo, E. Caminade, N. Joly, C. Madzak and C. Mougin, *Biochemistry*, 2002, **41**, 7325–7333; b) F. J. Enguita, D. Marçal, L. O. Martins, R. Grenha, A. O. Henriques, P. F. Lindley and M. A. Carrondo, *Journal of Biological Chemistry*, 2004, **279**, 23472–23476; c) E. Monza, M. F. Lucas, S. Camarero, L. C. Alejaldre, A. T. Martínez and V. Guallar, *J. Phys. Chem. Lett.*, 2015, **6**, 1447–1453.
35 C. C. S. Fortes, A. L. Daniel-da-Silva, A. M. R. B. Xavier and A. P. M. Tavares, *Chemical Engineering and Processing: Process Intensification*, 2017, **117**, 1–8.
36 a) S. K. S. Patel, V. C. Kalia, J.-H. Choi, J.-R. Haw, I.-W. Kim and J. K. Lee, *Journal of Microbiology and Biotechnology*, 2014, **24**, 639–647; b) H. Wang, W. Zhang, J. Zhao, L. Xu, C. Zhou, L. Chang and L. Wang, *Industrial & Engineering Chemistry Research*, 2013, **52**, 4401–4407; c) S. Rouhani, A. Rostami and A. Salimi, *RSC Adv.*, 2016, **6**, 26709–26718; d) J. N. Vranish, M. G. Ancona, S. A. Walper and I. L. Medintz, *Langmuir*, 2017, **34**, 2901-2925.
37 J. C. Cruz, P. H. Pfromm, J. M. Tomich and M. E. Rezac, *Colloids and Surfaces B: Biointerfaces,* 2010, **79**, 97–104.
38 a) F. Secundo, *Chemical Society Reviews*, 2013, **42**, 6250-6261; b) A. Arsalan and H. Younus, *International journal of biological macromolecules*, 2018, **118**, 1833–1847.
39 F.Yang, R. Backov, J-L. Blin, B. Fáklya, T. Tron, Y. Mekmouche, *Biotechnology Reports*, 2021, **31**, e00645.
40 C. A. Godoy, O. Romero, B. de las Rivas, C. Mateo, G. Fernandez-Lorente, J. M. Guisan, J. M. Palomo, *J. Mol. Cat. B: Enzymatic*, 2013, **87**, 121-127.
41 J. R. Simons, M. Mosisch, A. E. Torda, L. Hilterhaus, *J. Biotechnol.* 2013,**167**,1–7.
42 F. Liu, L. Wang, H. Wang, L. Yuan, J. Li, J. L. Brash, H. Chen, *ACS Appl. Mater. Interfaces,* 2015, **7**, 3717–3724.
43 Y. Li, T. L. Ogorzalek, S. Wei, X. Zhang, P. Yang, J. Jasensky, C. L. Brooks, III, E. Neil G. Marsh, Z. Chen, *Phys. Chem. Chem. Phys*., 2018, **20**, 1021-1029
44 R. Hong, T. Emrick and V. M. Rotello, *J. Am. Chem. Soc.*, 2004, **126**, 13572–13573.
45 a) A. A. Vertegel, R. W. Siegel, and J. S. Dordick, *Langmuir* 2004, **20**, 6800-6807; b) C. Rodriguez-Quijada, M. Sánchez-Purrà, H. de Puig, and K. Hamad-Schifferli, *J. Phys. Chem. B,* 2018, **122**, 2827–2840.
46 N. G. Lewis and L. B. Davin, in *Comprehensive Natural Products Chemistry*, Elsevier, 1999, pp. 639–712.